

Spin gating electrical current

C. Ciccarelli,¹ L. P. Zârbo,² A. C. Irvine,¹ R. P. Campion,³
B. L. Gallagher,³ J. Wunderlich,^{4,2} T. Jungwirth,^{2,3} and A. J. Ferguson¹

¹*Microelectronics Research Centre, Cavendish Laboratory,
University of Cambridge, CB3 0HE, United Kingdom*

²*Institute of Physics ASCR, v.v.i., Cukrovarnická 10, 162 53 Praha 6, Czech Republic*

³*School of Physics and Astronomy, University of Nottingham,
Nottingham NG7 2RD, United Kingdom*

⁴*Hitachi Cambridge Laboratory, Cambridge CB3 0HE, United Kingdom*

(Dated: January 15, 2019)

The majority of spintronic devices can be associated with one of two basic physical paradigms. The first stems from Mott's two-spin-channel picture of transport in ferromagnets with exchange-split bands¹ and the second is due to Dirac's quantum-relativistic spin-orbit coupling.² "Mott" devices, utilized in today's commercial spintronic sensors and memories, require at least two separate magnetic components and a spin current driven from one to the other component.³ "Dirac" devices, on the other hand, can rely on a single spin-orbit coupled component and spin current is not required to connect the spin-active component with another one. In our work we bring the distinction between "Mott" and "Dirac" paradigms to the fundamental level by demonstrating that "Dirac" spintronics can operate without any spin current. In other words, we show that in a spin sensitive transport device it is possible to remove the spin-orbit coupled component from the transport channel. We observe and microscopically explain an effect in which chemical potential shifts induced by rotated spins in a magnet control ordinary charge current in a capacitively coupled transport channel. The phenomenon provides a new concept for constructing spin transistors.

The archetype ohmic "Dirac" device is based on the relativistic anisotropic magnetoresistance (AMR) of a single magnetic conductor in which magnetization is rotated with respect to the current direction or crystal axes.³ The archetype ohmic "Mott" device is based on the giant-magnetoresistance (GMR) of a ferromagnet/normal-metal/ferromagnet tri-layer in which magnetizations in the ferromagnets are switched between parallel and anti-parallel configurations.³ In early 1990's the AMR and subsequently the GMR sensors were introduced in hard-drive read-heads launching the field of spintronics.³ In these ohmic devices, the spin-orbit coupled and the exchange-split bands enter the physics of spin transport in a complex way via electron scattering which is difficult to control. A more direct connection between spin dependent transport and band structure is realized in "Dirac" tunneling anisotropic magnetoresistance (TAMR)⁴⁻¹² and "Mott" tunneling magnetoresistance (TMR)³. These phenomena can be significantly larger than their ohmic counterparts; the large TMR signals are used, e.g., to represent logical 0 and 1 in magnetic random access memories.³

The work presented in this paper was inspired by the huge Coulomb blockade anisotropic magnetoresistance (CBAMR) of devices with a spin-orbit coupled magnet placed in a single-

electron transport channel.^{13–16} The magneto-transport response of these "Dirac" spintronic devices is coded in a single quantity derived directly from the relativistic band structure: the magnetization-orientation dependent chemical potential. Our spin gating phenomenon is based on removing the magnet with the tunable chemical potential from the transport channel and placing it in a capacitively-coupled gate electrode. As we show below, the spin state of the gate controls electrical current in a normal transport channel and, therefore, our "Dirac" spintronic device operates without spin current. The effect has no counterpart in "Mott" spintronics (For more details on the spin gating effect in the context of the two spintronics paradigms see Supplementary information).

To demonstrate the spin-gating phenomenon we use an aluminium single electron transistor (SET)¹⁷ with a ferromagnetic (Ga,Mn)As gate electrode. We choose an SET for this experiment due to its high charge sensitivity and (Ga,Mn)As for the gate electrode due to its well established relativistic magnetic anisotropy characteristics^{18,19}. We note, however, that spin-gating of any field effect device may be achieved. Placing the spin functionality in a magnetic gate allows the fabrication of spin sensitive devices with a variety of magnetic gates and with any desired non-magnetic material for the transistor channel.

Our SET has a micron-scale aluminium island separated by aluminium oxide tunnel junctions from source and drain leads (Fig. 1a). The aluminium is lightly doped with manganese to suppress superconductivity in our low-temperature (300 mK) measurements (see Supplementary information). The SETs are fabricated on top of epitaxially grown (Ga,Mn)As layers, which are electrically insulated from the SET by an alumina dielectric, and act as a spin-back-gate to the SET. The low total capacitance ($C_\Sigma \sim 0.6$ fF) of the island to its leads and back-gate yields a single-electron charging energy ($E_c = e^2/2C_\Sigma$) of ~ 100 μ eV.

By sweeping the externally applied potential to the SET gate (V_g) we obtain the conductance oscillations that characterize Coulomb blockade, as shown in Fig. 1b. The central result of our work is that in samples with magnetic gates we see a shift of these oscillations by an applied saturating magnetic field which rotates the magnetization in the (Ga,Mn)As gate. In Fig. 1b we show measurements for the in-plane ($\Phi = 90^\circ$) and for the perpendicular-to-plane ($\Phi = 0^\circ$) directions of magnetization. Alternatively, we plot in Fig. 1c the channel conductance as a function of the magnetization angle Φ for a fixed external potential V_g applied to the gate. The oscillations in Φ seen in Fig. 1c are of comparable amplitude as

the oscillations in V_g in Fig. 1b.

Due to the spin-orbit coupling, the band structure of (Ga,Mn)As is perturbed when its magnetisation \mathbf{M} is rotated. One consequence is a shift of the chemical potential, which in itself doesn't yield a response of the SET. However, the back-gate is attached to a charge reservoir so any change in the internal chemical potential of the gate causes an inward, or outward, flow of charge in the gate, as illustrated in Fig. 1e. This change in back-gate charge offsets the Coulomb oscillations (Fig. 1b) and changes the conductance of the transistor channel for a fixed external potential applied to the gate (Fig. 1c). Note that the absence of spin current removes the possibility of magneto-conductance artefacts due to spin accumulation, expected in the case that a spin current passes through the island of an SET. We also point out that the spin gating phenomenon observed in our SET with the (Ga,Mn)As back-gate is absent in a control sample with an identical SET channel and an Au gate electrode (see Supplementary information).

We now display the full experimental data sets for in-plane and out-of-plane magnetization rotations in a saturating magnetic field in the case of a ferromagnetic p-type $\text{Ga}_{0.97}\text{Mn}_{0.03}\text{As}$ gate (Fig. 2a,b). We fit a sinusoid to the Coulomb oscillations and extract the resulting gate-voltage offset (ΔV_g) as a function of the magnetization angle. A positive value of ΔV_g means that, for a fixed gate voltage, holes leave the gate, which can be attributed to an increased hole chemical potential, $\Delta\mu=e\Delta V_g$.

The anisotropy of $\Delta\mu$ for out-of-plane rotation of \mathbf{M} has a uniaxial symmetry ($\Delta\mu_{\Phi}^u=81\ \mu\text{eV}$) (Fig. 2c), whereas the in-plane rotation anisotropy is predominantly uniaxial ($\Delta\mu_{\theta}^u=30\ \mu\text{eV}$) with a small cubic component ($\Delta\mu_{\theta}^c=6\ \mu\text{eV}$) (Fig. 2d). The $\Delta\mu$ anisotropy is greater for the out-of-plane rotation, and causes a shift in the Coulomb oscillations by a quarter of a period. We also measured SETs with a $\text{Ga}_{0.94}\text{Mn}_{0.06}\text{As}$ back-gate (Figs. 2e,f). The magnitude of both the out-of-plane rotation ($\Delta\mu_{\Phi}^u=144\ \mu\text{eV}$) and the in-plane rotation ($\Delta\mu_{\theta}^u=46\ \mu\text{eV}$) uniaxial anisotropies increase in the sample with higher Mn concentration while the in-plane cubic anisotropy component is negligibly small in the $\text{Ga}_{0.94}\text{Mn}_{0.06}\text{As}$ sample. The chemical potential anisotropy constants are consistent between samples fabricated from the same MBE grown wafers. This is because the spin gating phenomenon measures the properties of the material surface (over a $\sim\ \mu\text{m}^2$ area in our sample) rather than the properties of a specific nano-device as reported in the measurements of CBAMR.¹³⁻¹⁶

We repeated field rotation measurements for different values of the saturating field, observing only a weak dependence of the $\Delta\mu$ anisotropy components on the field magnitude (Fig. 3a). This confirms that the origin of the observed spin-gating is the anisotropy of the chemical potential in the ferromagnetic gate with respect to the magnetization orientation. (Recall that the effective g-factor in the GaAs valence band has a negligible anisotropy.²⁰)

The chemical potential anisotropy origin of the observed spin-gating effect is confirmed by microscopic calculations based on the $\mathbf{k} \cdot \mathbf{p}$ kinetic-exchange model of (Ga,Mn)As^{21,22} (see (Figs. 3b,c) and Supplementary information). We have calculated chemical potential anisotropies for the out-of-plane magnetization rotation assuming local Mn moment concentrations and lattice-matching growth strains corresponding to the measured (Ga,Mn)As samples. We consider one hole per Mn_{Ga} local moment (Mn_{Ga} is a single acceptor), as well as cases with partial hole depletion. The latter calculations were performed since the spin-gating experiments are sensitive to the partially depleted surface layer which has a width given by the hole screening length (a few nm).

In agreement with experiment, we find theoretical chemical potential anisotropies of the order of 10-100 μeV . The calculated enhancement of the chemical potential anisotropy with increasing local moment concentration and lattice-matching growth strain is also consistent with the enhanced spin-gating effect observed experimentally in the Ga_{0.94}Mn_{0.06}As sample as compared to the Ga_{0.97}Mn_{0.03}As sample. We also note that the increase in the higher Mn-doped sample of the measured and calculated chemical potential anisotropy for the out-of-plane rotation is consistent with the doping trends in the corresponding magnetocrystalline anisotropy coefficient of (Ga,Mn)As²³. Similarly, the measured enhancement of the in-plane uniaxial component of the chemical potential anisotropy and the suppression of the cubic component in the higher Mn-doped sample is consistent with the corresponding magnetocrystalline anisotropy trends²³. The microstructural origin of the in-plane uniaxial anisotropy component is not established and to capture this component one can, e.g., introduce an effective shear strain in the $\mathbf{k} \cdot \mathbf{p}$ Hamiltonian which breaks the [110]/[1-10] crystal symmetry.^{23,24} The values of the shear strain required to reproduce the in-plane uniaxial magnetocrystalline anisotropy yield a corresponding chemical potential anisotropy of the order of $\sim 10 - 100 \mu\text{eV}$, again consistent with our measured data. Similar to the established phenomenology of the spin-orbit coupling induced magnetocrystalline anisotropies, or ohmic and tunneling AMRs, the sign of the chemical potential anisotropy is not strictly

determined by the sign of the strain and by other symmetries of the crystal, and may vary when changing the local moment or hole concentration in (Ga,Mn)As. We note that the agreement in the sign of the theoretical and experimental chemical potential anisotropy is obtained assuming partially depleted holes, consistent with the expected sensitivity in our device to the (Ga,Mn)As surface layer.

We conclude by pointing out that our work inverts the conventional spin transistor: instead of spin-transport controlled by ordinary gates we spin-gate ordinary charge transport. Our approach can be used to catalogue spin gating phenomena in a variety of magnetic materials, simply by exchanging the gate electrode. Chemical potential shifts of the order of 1-10 meV's are predicted, e.g., for several ferromagnetic and antiferromagnetic transition metal alloys.^{13,25} We also point out that our concept removes a major road block for spintronics technologies which is the presence of spin-sensitive (magnetic) elements in the transport channel compromising its electrical performance. With spin gating, any desired non-magnetic material can be used for the transistor channel. For example, the electrical current flowing through a high-mobility field effect transistor could be used to determine the magnetic state of its gate, providing a new read-out concept for a magnetic memory device and opening a route to the realization of hybrid transistor-memory elements. The control of electron transport by internal chemical potential shifts in the gate electrode, demonstrated in our work for a magnetically ordered gate, is a generic phenomenon applicable also to variations of other order parameters that may be present in physical systems.

¹ Mott, N. F. The electrical conductivity of transition metals. *Proc. R. Soc. Lond. A* **153**, 699 (1936).

² Strange, P. *Relativistic Quantum Mechanics* (Cambridge University Press, 1998).

³ Chappert, C., Fert, A. & Dau, F. N. V. The emergence of spin electronics in data storage. *Nature Mat.* **6**, 813 (2007).

⁴ Gould, C. *et al.* Tunneling anisotropic magnetoresistance: A spin-valve like tunnel magnetoresistance using a single magnetic layer. *Phys. Rev. Lett.* **93**, 117203 (2004).

⁵ Brey, L., Tejedor, C. & Fernández-Rossier, J. Tunnel magneto-resistance in GaMnAs: going beyond Julliere formula. *Appl. Phys. Lett.* **85**, 1996 (2004).

- ⁶ Giraud, R., Gryglas, M., Thevenard, L., Lemaître, A. & Faini, G. Voltage-controlled tunneling anisotropic magneto-resistance of a ferromagnetic p++ (Ga,Mn)As / n+ GaAs Zener-Esaki diode. *Appl. Phys. Lett.* **87**, 242505 (2005).
- ⁷ Sankowski, P., Kacman, P., Majewski, J. A. & Dietl, T. Spin-dependent tunneling in modulated structures of (Ga,Mn)As. *Phys. Rev.* **B 75**, 045306 (2007).
- ⁸ Ciorga, M., Einwanger, A., Sadowski, J., Wegscheider, W. & Weiss, D. Tunneling anisotropic magnetoresistance effect in a p+ (Ga,Mn)As/n+ GaAs Esaki diode. *Phys. Stat. Sol A* **204**, 186 (2007).
- ⁹ Moser, J. *et al.* Tunneling anisotropic magnetoresistance and spin-orbit coupling in Fe/GaAs/Au tunnel junctions. *Phys. Rev. Lett.* **99**, 056601 (2007).
- ¹⁰ Gao, L. *et al.* Bias voltage dependence of tunneling anisotropic magnetoresistance in magnetic tunnel junctions with MgO and Al₂O₃ tunnel barriers. *Phys. Rev. Lett.* **99**, 226602 (2007).
- ¹¹ Park, B. G. *et al.* Tunneling anisotropic magnetoresistance in multilayer-(Co/Pt)/AlO_x/Pt structures. *Phys. Rev. Lett.* **100**, 087204 (2008).
- ¹² Park, B. G. *et al.* A spin-valve-like magnetoresistance of an antiferromagnet-based tunnel junction. *Nature Mat.* **10**, 347 (2011).
- ¹³ Wunderlich, J. *et al.* Coulomb blockade anisotropic magnetoresistance effect in a (Ga,Mn)As single-electron transistor. *Phys. Rev. Lett.* **97**, 077201 (2006).
- ¹⁴ Wunderlich, J. *et al.* Ordinary and extraordinary coulomb blockade magnetoresistance in (Ga,Mn)As single electron transistor. *Solid State Commun.* **144**, 536 (2007).
- ¹⁵ Schlapps, M. *et al.* Transport through (Ga,Mn)As nanoislands: Coulomb blockade and temperature dependence of the conductance. *Phys. Rev.* **B 80**, 125330 (2009).
- ¹⁶ Bernand-Mantel, A. *et al.* Anisotropic magneto-coulomb effects and magnetic single-electron-transistor action in a single nanoparticle. *Nat. Phys.* **5**, 920 (2009).
- ¹⁷ Likharev, K. K. Single-electron devices and their applications. *Proceedings of the IEEE* **87**, 606 (1999).
- ¹⁸ Jungwirth, T., Sinova, J., Mašek, J., Kučera, J. & MacDonald, A. H. Theory of ferromagnetic (III,Mn)V semiconductors. *Rev. Mod. Phys.* **78**, 809 (2006).
- ¹⁹ Dietl, T., Awschalom, D. D., Kaminska, M., Ohno, H. (eds.), Spintronics. *Semiconductors and Semimetals* **82** (Elsevier, 2008).
- ²⁰ Winkler, R. Rashba spin splitting in two-dimensional electron and hole systems. *Phys.Rev.* **B**

62, 4245 (2000).

- ²¹ Dietl, T., Ohno, H. & Matsukura, F. Hole-mediated ferromagnetism in tetrahedrally coordinated semiconductors. *Phys. Rev. B* **63**, 195205 (2001).
- ²² Abolfath, M., Jungwirth, T., Brum, J. & MacDonald, A. H. Theory of magnetic anisotropy in $\text{III}_{1-x}\text{Mn}_x\text{V}$ ferromagnets. *Phys. Rev. B* **63**, 054418 (2001).
- ²³ Zemen, J., Kucera, J., Olejnik, K. & Jungwirth, T. Magneto crystalline anisotropies in (Ga,Mn)As: A systematic theoretical study and comparison with experiment. *Phys. Rev. B* **80**, 155203 (2009).
- ²⁴ Sawicki, M. *et al.* In-plane uniaxial anisotropy rotations in (Ga,Mn)As thin films. *Phys. Rev. B* **71**, 121302 (2005).
- ²⁵ Shick, A. B., Khmelevskiy, S., Mryasov, O. N., Wunderlich, J. & Jungwirth, T. Spin-orbit coupling induced anisotropy effects in bimetallic antiferromagnets: A route towards antiferromagnetic spintronics. *Phys. Rev. B* **81**, 212409 (2010).

Corresponding author

Correspondence and requests for materials should be addressed to A.J.F, ajf1006@cam.ac.uk, Microelectronics Group, Cavendish Laboratory, University of Cambridge, CB3 0HE, United Kingdom

Acknowledgment

We acknowledge support from EU Grants FP7-214499 NAMASTE, FP7-215368 SemiSpinNet, ERC Advanced Grant, from Czech Republic Grants AV0Z10100521, KAN400100652, KJB100100802 and Preamium Academiae, A.J.F. acknowledges the support of a Hitachi research fellowship.

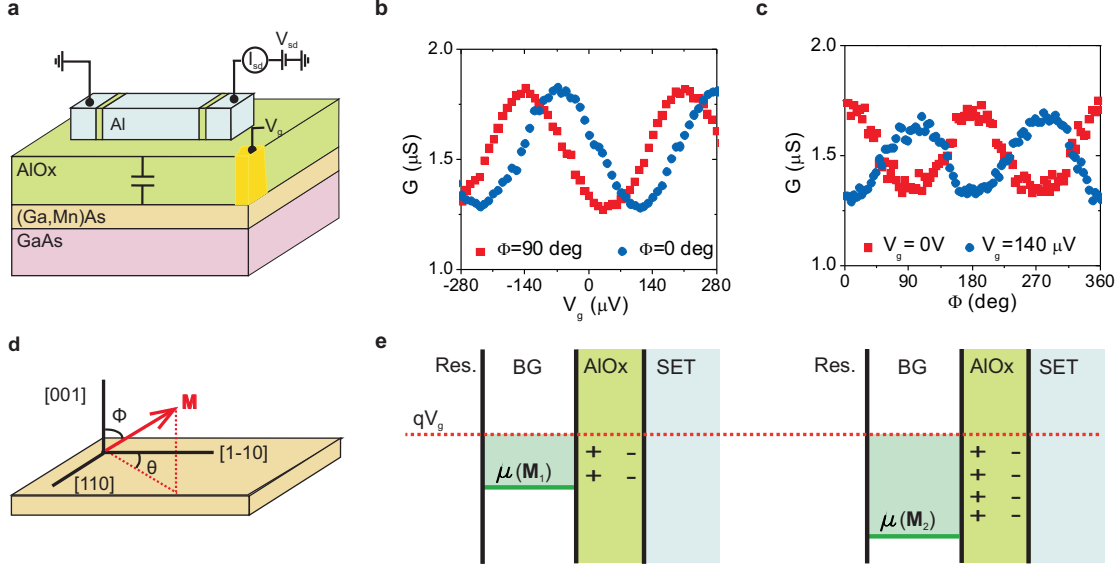


Figure 1: Observation of the spin gating effect. **a**, Schematic showing our SET channel separated by AlO_x dielectric from the ferromagnetic $(\text{Ga,Mn})\text{As}$ back-gate. The SET comprises Al leads and island, and AlO_x tunnel barriers (a micrograph can be found in the supplementary information). **b**, Coulomb oscillations in externally applied gate voltage for the SET on $\text{Ga}_{0.97}\text{Mn}_{0.03}\text{As}$ for two different polar angles Φ of the magnetisation. **c**, Magneto-Coulomb oscillations shown by the same SET by varying the angle of magnetisation for two different gate voltages. Measurements were performed using a low frequency lock-in technique with excitation voltage $20 \mu\text{V}$ and dc offset voltage $V_{sd} = 0$. **d** Magnetisation vector with respect to $(\text{Ga,Mn})\text{As}$ crystal axes. **e**, Schematic explaining the spin gating phenomenon: reorientation of the magnetisation from \mathbf{M}_1 to \mathbf{M}_2 causes a change in the chemical potential of the $(\text{Ga,Mn})\text{As}$ back-gate (BG). This causes charge to flow onto the back-gate from the reservoir (Res.). The net effect is to alter the charge on the back-gate and therefore the SET conductance. We show a decrease in hole chemical potential μ between \mathbf{M}_1 and \mathbf{M}_2 . The externally applied electrochemical potential on the gate $\mu_{ec} = eV_g$ is held constant.

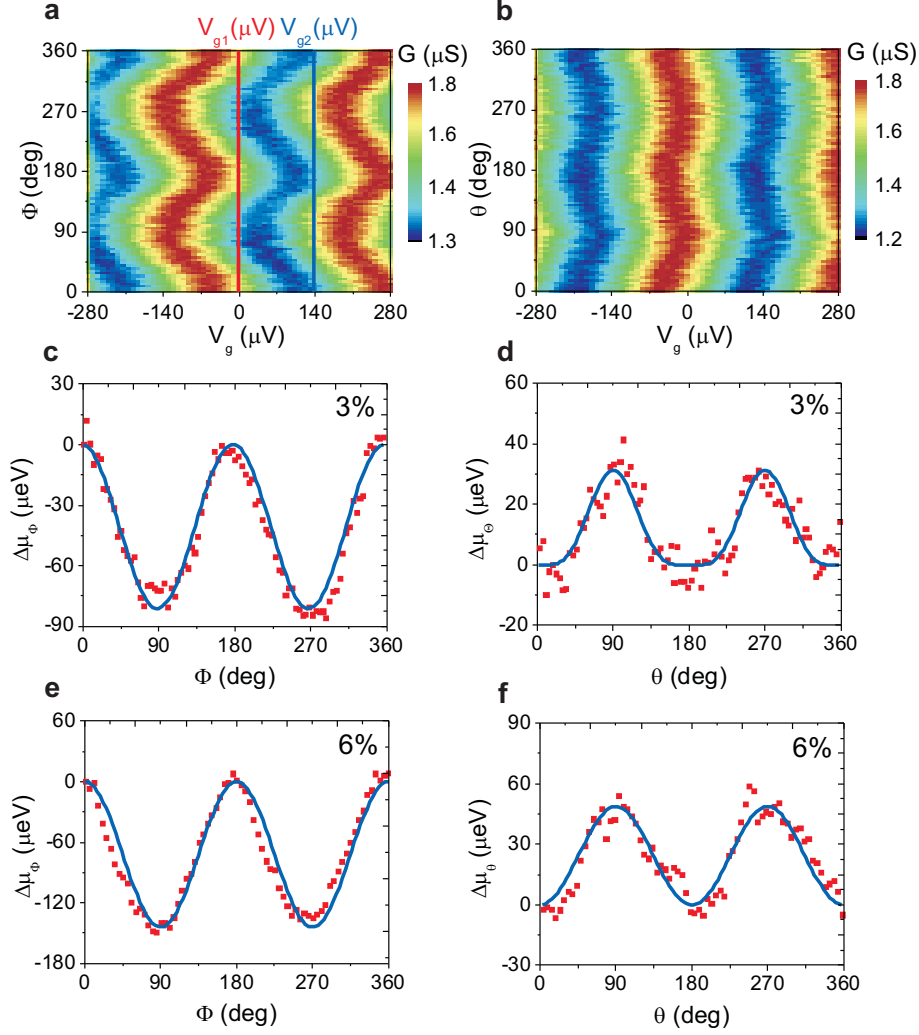


Figure 2: Magneto-Coulomb oscillations and chemical potential shifts. **a**, SET conductance measurements for azimuthal angle $\theta = 0$ as a function of the out-of-plane polar angles Φ of the $\text{Ga}_{0.97}\text{Mn}_{0.03}\text{As}$ magnetisation and of the gate voltage. The magnetisation is rotated by a 1 T magnetic field. The two lines represent the gate voltage offsets for the data shown in Fig. 1c. **b**, Measurements with in-plane rotation of magnetisation for the same sample. The magnetisation is rotated by a 0.8 T magnetic field. **c**, $\text{Ga}_{0.97}\text{Mn}_{0.03}\text{As}$ hole chemical potential shift ($\Delta\mu_{\Phi} = \mu(\Phi) - \mu(\Phi = 0)$) for the out-of-plane magnetisation rotation, inferred from measurements in **a**. **d**, $\text{Ga}_{0.97}\text{Mn}_{0.03}\text{As}$ hole chemical potential shift ($\Delta\mu_{\theta} = \mu(\theta) - \mu(\theta = 0)$) for the in-plane magnetisation rotation, inferred from measurements in **b**. **e,f**, Hole chemical potential shifts for the $\text{Ga}_{0.94}\text{Mn}_{0.06}\text{As}$ gate electrode. The data (red squares) are fitted (blue lines) to extract the uniaxial and cubic contributions to the $\Delta\mu$ anisotropy.

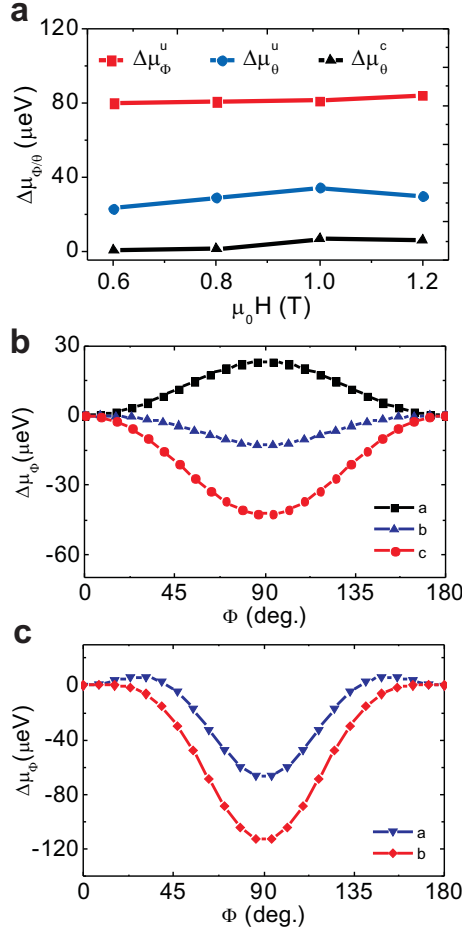


Figure 3: Experimental and theoretical chemical potential anisotropies.

a, Experimental values for cubic and uniaxial contributions to the $\Delta\mu$ anisotropy, measured for different saturation fields, for the $\text{Ga}_{0.97}\text{Mn}_{0.03}\text{As}$ gate material. **b**, Theoretical variations of the chemical potential with respect to the magnetization angle Φ for fixed Mn moment density $N_{\text{Mn}} = 4.4 \times 10^{20} \text{cm}^{-3}$ (corresponding approximately to the measured sample with 3% nominal doping) and compressive growth strain $\epsilon_0 = -0.3\%$. The hole density $p = N_{\text{Mn}}$, $p = 0.4N_{\text{Mn}}$ and $p = 0.2N_{\text{Mn}}$ for curves a, b, and c, respectively. **c**, Theoretical chemical potential anisotropies for $N_{\text{Mn}} = 8.8 \times 10^{20} \text{cm}^{-3}$ (corresponding approximately to the measured sample with 6% nominal doping) and charge density $p = 0.2N_{\text{Mn}}$. The curve a is for the strain $\epsilon_0 = -0.3\%$ while curve b is for $\epsilon_0 = -0.5\%$.